Long-Term Correlations in the Spike Trains of Medullary Sympathetic Neurons

CRAIG D. LEWIS, GERARD L. GEBBER, PETER D. LARSEN, AND SUSAN M. BARMAN
Department of Pharmacology and Toxicology, Michigan State University, East Lansing, Michigan 48824-1317

Received 21 August 2000; accepted in final form 2 January 2001

Lewis, Craig D., Gerard L. Gebber, Peter D. Larsen, and Susan M. Barman. Long-term correlations in the spike trains of medullary sympathetic neurons. *J Neurophysiol* 85: 1614–1622, 2001. Fano factor analysis was used to characterize the spike trains of single medullary neurons with sympathetic nerve–related activity in cats that were decerebrate or anesthetized with Dial-urethan or urethan. For this purpose, values (Fano factor) of the variance of the number of extracellularly recorded spikes divided by the mean number of spikes were calculated for window sizes of systematically varied length. For window sizes ≤10 ms, the Fano factor was close to one, as expected for a Bernoulli process with a low probability of success. The Fano factor dipped below one as the window size approached the shortest interspike interval (ISI) and reached its nadir at window sizes near the modal ISI. The extent of the dip reflected the shape (skewness) of the ISI histogram with the dip being smallest for the most asymmetric distributions. Most importantly, for a wide range of window sizes exceeding the modal ISI, the Fano factor curve took the form of a power law function. This was the case independent of the component (cardiac related, 10 Hz, or 2–6 Hz) of inferior cardiac sympathetic nerve discharge to which unit activity was correlated or the medullary region (lateral tegmental field, raphe, caudal and rostral ventrolateral medulla) in which the neuron was located. The power law relationship in the Fano factor curves was eliminated by randomly shuffling the ISIs even though the distribution of the intervals was unchanged. Thus the power law relationship arose from long-term correlations among ISIs that were disrupted by shuffling the data. The presence of long-term correlations across different time scales reflects the property of statistical self-similarity that is characteristic of fractal processes. In most cases, we found that mean ISI and variance for individual spike trains increased as a function of the number of intervals counted. This can be attributed to the clustering of long and short ISIs, which also is an inherent property of fractal time series. We conclude that the spike trains of brain stem sympathetic neurons have fractal properties.

INTRODUCTION

As demonstrated with spike-triggered averaging and coherence analysis, the naturally occurring activity of single neurons in four regions of the cat medulla have been found to be correlated to one or more of the rhythmic components in postganglionic sympathetic nerve discharge (SND) (Barman and Gebber 1983, 1985, 1987, 1989, 1992, 1997; Barman et al. 1994, 1995). The regions containing these neurons are the rostral ventrolateral medulla (RVLM), caudal medullary raphe nuclei, medullary lateral tegmental field (LTF), and caudal ventrolateral medulla (CVLM). The neurons in the RVLM and medullary raphe send their axons to the thoracic spinal intermediolateral nucleus (IML) and receive converging inputs from the generators of the cardiac-related and 10-Hz rhythms and the irregular 2- to 6-Hz oscillations in SND. Those in the LTF and CVLM do not project to the spinal cord. The LTF neurons have activity correlated to the cardiac-related and 2- to 6-Hz bursts in SND but not the 10-Hz rhythm, while the CVLM contains a population of cells with activity correlated only to the 10-Hz rhythm. Correlation of medullary unit activity to SND results in statistically significant linear coherence, but the relationship is far less than perfect (i.e., unit-SND coherence values usually fall well below 1.0). At least two factors account for the less than perfect relationship. First, the interval between medullary unit spike occurrence and the rhythmic burst of SND is not absolutely fixed. Second, with rare exception, the neurons do not fire during every cycle of rhythmic SND, and the number of cycles between successive spikes is highly variable. As a consequence, their interspike intervals (ISIs) either approximate a gamma distribution with a long tail or are multimodal (Barman and Gebber 1992).

The current study was initiated to define the basis for the highly variable ISIs of medullary neurons with sympathetic nerve–related activity. We considered two alternative hypotheses. First, the variability of ISIs is best described by a renewal process in which the intervals are independent of each other (Cox and Lewis 1966; Tuckwell 1988). In this case, the spike train approximates a stochastic point process. The second hypothesis is that there are long-term correlations among ISIs indicative of a fractal point process.

A fractal spike train is statistically self-similar in that fluctuations in ISIs and other properties measured over brief times are proportional to those measured over longer times. Because the features measured at different temporal resolutions are related, self-similarity implies that long-term correlations exist among the ISIs (Bassingthwaighte et al. 1994; Teich 1992; West 1990). How the measured properties of a fractal time series depend on the resolution used to make the measurement is called the scaling relationship. The simplest scaling relationship determined by self-similarity has a power law form. Power law scalings are reflected by a straight line on a log-log plot relating the variable measured to the resolution used to make the measurement. Although not all power law relationships are due to fractals, the appearance of such a relationship should encourage the use of tests to determine whether the time

Address reprint requests to G. L. Gebber (E-mail: gebber@msu.edu).

The costs of publication of this article were defrayed in part by the payment of page charges. The article must therefore be hereby marked "*advertisement*" in accordance with 18 U.S.C. Section 1734 solely to indicate this fact.

series is statistically self-similar and thus fractal in nature. In the current study we used one such test, Fano factor analysis (Teich 1992), to examine the spike trains of single neurons in the cat medulla with activity correlated to the discharges of the inferior cardiac postganglionic sympathetic nerve.

METHODS

General procedures and recordings

The data analyzed were available from earlier studies from this laboratory (Barman and Gebber 1983, 1985, 1987, 1989, 1992, 1997; Barman et al. 1994, 1995). The experiments were performed in baroreceptor-intact or -denervated cats that were unanesthetized and decerebrated at the midcollicular level, or anesthetized with either urethan (1.2–1.8 g/kg iv) or a mixture of sodium diallylbarbiturate (60 mg/kg), urethan (240 mg/kg), and monoethylurea (240 mg/kg) administered intraperitoneally, henceforth referred to as Dial-urethan. Baroreceptor denervation was performed by bilateral section of the carotid sinus, aortic depressor, and vagus nerves. Blood pressure was recorded from either the femoral or brachial artery. All of the experimental procedures were approved by the All-University Committee on Animal Use and Care of Michigan State University.

The methods used to make extracellular recordings of the discharges of single medullary neurons and population activity of the postganglionic inferior cardiac sympathetic nerve are described in detail in the original reports. Action potentials of individual neurons (preamplifier band-pass, 300–3,000 Hz) were isolated from background by using analog window discrimination. The criteria used to establish the unitary nature of the recordings can be found in the original reports. Postganglionic SND was recorded with a preamplifier band-pass of 1–1,000 Hz. The synchronized discharges of sympathetic fibers appear as slow waves (envelopes of spikes) under these conditions (Cohen and Gootman 1970; Gebber et al. 1999).

Data analysis

Standardized square-wave pulses representing the action potentials of single medullary neurons were used as references to construct spike-triggered averages of SND (resolution, 2 ms/bin) with software from RC Electronics (Santa Barbara, CA). A series of randomly generated pulses with the same mean frequency as the neuronal spike train was used to construct a "dummy" average of SND from the same data block. The discharges of medullary neurons were considered to be correlated to SND if the amplitude of the peak near *time 0* (coincident with unit discharge) in the spike-triggered average was at least three times that of the largest deflection in the dummy average.

Software written by Lewis (see Gebber et al. 1999) was used to detect the pulses representing unit action potentials and to measure ISIs (resolution, 1 ms). Time series of the ISIs, interspike interval histograms (ISIHs), and Fano factor curves were constructed from these events. The Fano factor, $F(T)$ as used by Teich (1992) is defined as the variance (var) of the number of spikes divided by the mean number of spikes for a given time window of length T

$$F(T) = \frac{\text{var}\,[N_i(T)]}{\text{mean}\,[N_i(T)]}$$

where $N_i(T)$ is the number of spikes in the ith window of length T. A curve is constructed by plotting the Fano factor as a function of the window size on a log-log scale. For a total data block of length T_{max}, the window size, T, is varied from a minimum of 1 ms to a maximum of $T_{max}/10$, so that at least 10 nonoverlapping windows were used for each measure of the Fano factor. For a renewal process in which the ISIs are uncorrelated, the variance-to-mean spike count ratio (i.e., Fano factor) is one for all window sizes (Koch 1999). For a periodic (rhythmic) process, the variance decreases and the Fano factor approaches zero as the window size is increased (Bassingthwaighte et al. 1994). For a fractal process, the Fano factor increases as a power of the window size and may reach values >1.0. This reflects the greater variance of spike counts with increasing window size. The increase in the variance occurs because rarer clusters of long and short ISIs are more apt to be found as more and more data are collected. Such clustering is characteristic of a fractal process (Teich 1989). The power law relationship between the Fano factor and window size is manifested by a straight line with a positive slope on a log-log plot. The slope, which is referred to as the scaling exponent, is the power to which the fluctuations of spike counts on one scale are proportional to those on longer scales. Regression analysis was used to calculate the slope of the power law relationship, and the correlation coefficient (r value) was used as a test for linearity.

Whether a power law relationship in the Fano factor curve reflects statistical self-similarity, and thus long-term correlations among ISIs, is tested by constructing surrogate data sets. For this purpose, the ISIs in the original spike train are randomly shuffled. Shuffling creates a time series whose mean ISI, ISI variance, and ISIH are identical to those of the original spike train, but with no correlations among the ISIs (Teich and Lowen 1994; Teich et al. 1996). If shuffling eliminates the power law relationship, it can be concluded that long-term correlations existed in the original data set. We routinely compared the Fano factor curve for the original spike train with those for 10 independently constructed surrogate data sets.

RESULTS

Relationships between medullary unit activity and SND

Medullary neurons with activity correlated to the cardiac-related rhythm in inferior cardiac SND were identified in baroreceptor-intact cats that were decerebrate or anesthetized either with urethan or Dial-urethan. A typical example is shown in Fig. 1*A*. The traces on the *left* show from *top* to *bottom*, the arterial pulse (AP), inferior cardiac SND, and standardized pulses representing the spikes of an RVLM neuron. Although the RVLM neuron did not discharge during every cardiac-related burst of SND, unit activity was correlated to the sympathetic nerve slow wave. This was formally demonstrated by spike-triggered averaging of SND (Fig. 1*A*, *right*). Note that the amplitude of the slow waves in the spike-triggered average (STA) exceeded those of the deflections in the dummy average by a factor greater than three, and that unit activity was most apt to occur near the start of the rising phase of the cardiac-related sympathetic nerve slow wave.

Medullary unit activity correlated to the 10-Hz rhythm in SND was observed in baroreceptor-denervated cats that were decerebrate or anesthetized with urethan. An example of this type of relationship is shown in Fig. 1*B*. As was the case for the cardiac-related rhythm, this RVLM neuron did not discharge during every 10-Hz burst of SND (Fig. 1*B*, *left*). The spike-triggered average (Fig. 1*B*, *right*) shows that unit activity was most apt to occur at the start of the rising phase of the 10-Hz slow wave in SND.

Noncardiac-related 2- to 6-Hz oscillations appear in place of the 10-Hz rhythm in baroreceptor-denervated cats anesthetized with Dial-urethan (Kocsis et al. 1990). In the example shown in Fig. 1*C*, RVLM unit activity was correlated to this component in SND. The traces on the left illustrate the absence of 1:1 locking of SND to the arterial pulse and the variability of ISIs of the RVLM unit. The spike-triggered average for this unit shows one large peak near zero lag. In this case, the RVLM neuron was most apt to discharge during the early rising phase

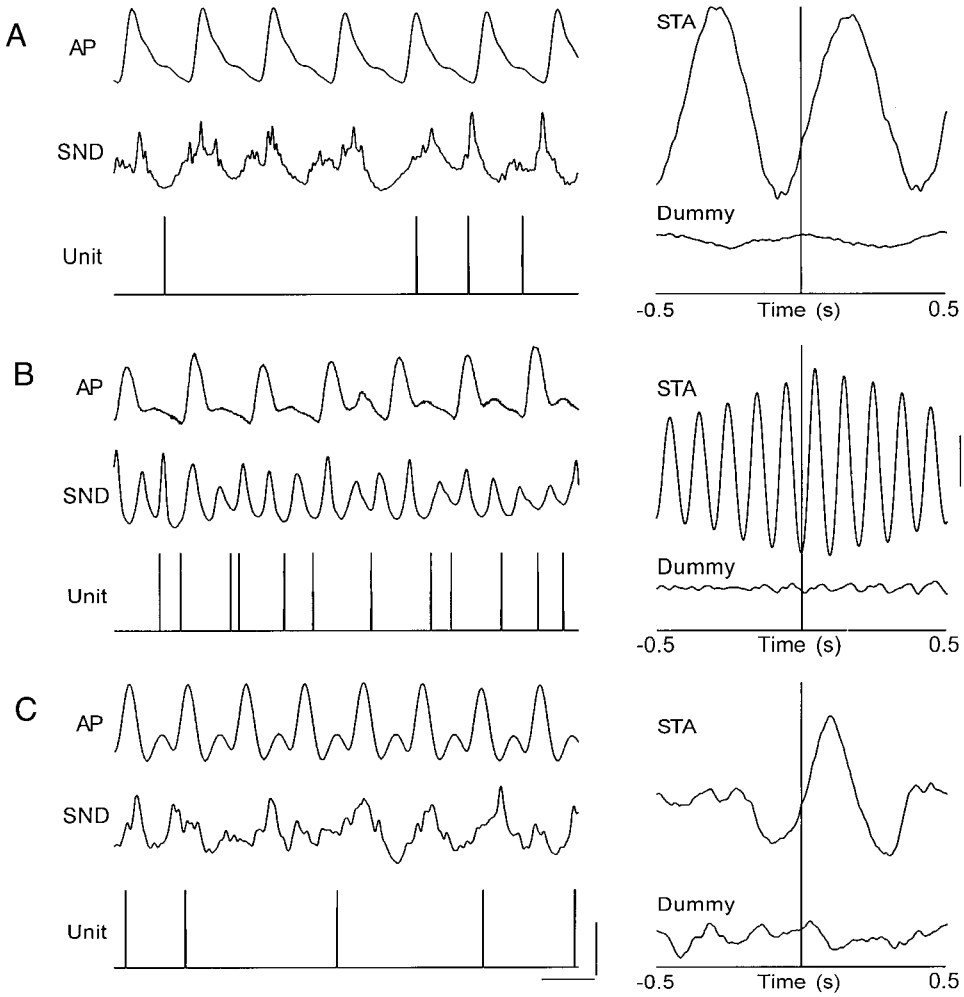

FIG. 1. Time-domain analysis of relationships between the extracellularly recorded action potentials of single neurons in the rostral ventrolateral medulla (RVLM) and postganglionic inferior cardiac sympathetic nerve discharge (SND). *A–C*: traces on the *left* (*top* to *bottom*) are arterial pulse (AP), original recording of SND, and standardized pulses representing RVLM unit spikes. Vertical calibration refers to SND and is 100 μV in *A*, 150 μV in *B*, and 80 μV in *C*. Horizontal calibration is 67 ms. Traces on the *right* are spike-triggered average (STA; *top*) and "dummy" pulse-triggered average (*bottom*) of SND. Number of trials averaged was 1,459 in *A*, 3,189 in *B*, and 2,429 in *C*. Unit activity is correlated to the cardiac-related rhythm in *A*, 10-Hz rhythm in *B*, and irregular 2- to 6-Hz oscillations in *C*. Vertical calibration is 20 μV in *A*, 25 μV in *B*, and 15 μV in *C*.

of the 2- to 6-Hz slow wave in SND. The absence of large secondary peaks in the spike-triggered average was expected because inter-slow wave intervals vary considerably in the 2- to 6-Hz band.

Spike trains of neurons with sympathetic nerve–related activity

We analyzed the spike trains of 92 medullary neurons with sympathetic nerve–related activity. Those with activity correlated to the cardiac-related rhythm in SND included 11 RVLM neurons, 18 LTF neurons, and 8 raphe neurons. Those with activity correlated to the 10-Hz rhythm included 11 RVLM neurons, 9 raphe neurons, and 8 CVLM neurons. Those with activity correlated to irregular 2- to 6-Hz oscillations in SND included 12 RVLM neurons, 9 LTF neurons, and 6 raphe neurons.

The results obtained for an RVLM neuron with activity correlated to the 10-Hz rhythm in SND (baroreceptor-denervated cat) are shown in Fig. 2*A*. The ISIs for this neuron are plotted as a time series in the *top panel*. The time series was 564 s in length and contained 681 spikes. Note the clustering of relatively long intervals and of shorter intervals. Such clustering is characteristic of statistically self-similar processes (Bassingthwaighte et al. 1994; Liebovitch 1998). The ISIH was gamma-like in shape with a long tail reaching 7 s (Fig. 2*A*, *middle*). The shortest ISI was 51 ms, and the modal ISI was 230 ms (approximately twice the period of the 10-Hz rhythm in SND). The coefficient of variation (CV; SD/mean ISI) was 0.94. Figure 2*A*, *bottom*, shows the Fano factor curve for the spike train (black line). For very small window sizes ($\leq$10 ms) the Fano factor was close to one. This standard feature of the Fano factor curve is consistent with a Bernoulli process with a low probability of success (Teich 1992). This is explained by the fact that, for window sizes much smaller than the shortest ISI, the spike count can be either zero or one, with the former outcome more likely to occur. For window sizes approaching the shortest ISI, the Fano factor dipped below one and reached its lowest value at window sizes near the modal ISI. As a general rule, the extent of the dip reflects the shape (skewness) of the ISIH (Teich 1992). As was the case in Fig. 2*A*, the dip is relatively small for a highly skewed (asymmetric) ISIH. Note that the Fano factor curve for the original spike train is indistinguishable from those for the surrogate data sets (Fig. 2*A*, *bottom*, gray region) at window sizes close to the modal ISI. This was expected because random shuffling of the ISIs does not change the shape of the ISIH (Teich and Lowen 1994; Teich et al. 1996).

In Fig. 2*A*, *bottom*, for window sizes $>$2 s, the Fano factor for the RVLM spike train exceeded a value of one, and the curve took the form of a power law with a positive slope

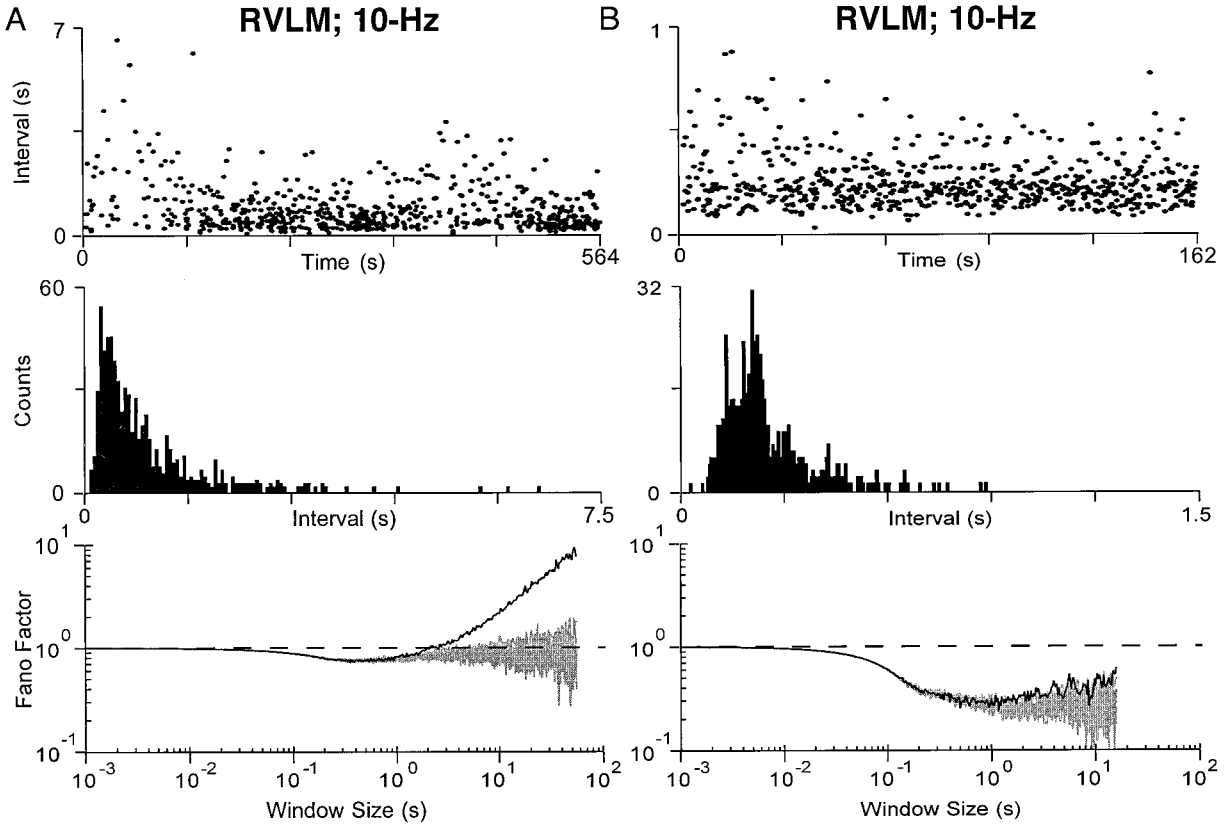

FIG. 2. Fano factor analysis of the spike trains of 2 RVLM neurons (*A* and *B*) with activity correlated to the 10-Hz rhythm in inferior cardiac SND. Traces (*top* to *bottom*) are time series of interspike intervals (ISIs), interspike interval histograms (ISIHs), and Fano factor curves. Total counts in ISIHs is 680 in *A* and 673 in *B*. The shortest and modal ISIs were 51 and 230 ms, respectively, in *A* and 27 and 210 ms in *B*. Bin resolution (ISIHs) is 50 ms in *A* and 10 ms in *B*. Black line is Fano factor curve for original spike train. Gray region is the superposition of the curves for 10 surrogate data sets.

(scaling exponent) of 0.79. The power law relationship in the Fano factor curve suggests that long-term correlations existed among the ISIs. This was shown to be the case by shuffling the ISIs. Note the absence of power law relationships (i.e., essentially flat slope) in the curves for the surrogate data sets at window sizes >2 s.

The results for another RVLM neuron with activity correlated to the 10-Hz rhythm are shown in Fig. 2*B*. The time series was 162 s in length and contained 674 spikes (Fig. 2*B*, *top*). The shortest ISI was 27 ms, and the modal ISI was 210 ms. Note that the ISIH (Fig. 2*B*, *middle*) was less skewed (CV = 0.50) relative to the example in Fig. 2*A*. Thus the spike train more closely approached a rhythmic process. As such, the dip in the Fano factor at window sizes near the modal ISI was quite pronounced, and the Fano factor remained below one at the largest window size that satisfied the 10 windows criterion for calculation (Fig. 2*B*, *bottom*, dark line). At no point did the Fano factor curve for the spike train diverge from the spread of the curves for the surrogate data blocks (Fig. 2*B*, *bottom*, gray region). Thus long-term correlations among the ISIs could not be demonstrated for this RVLM neuron.

Independent of the region in which the medullary unit was located or the component of SND to which its activity was correlated, the Fano factor curve always exhibited a power law relationship for window sizes generally ≥1 s when the time series contained ≥2,000 spikes (n = 19). In fact, the Fano factor curve for only 1 unit (an LTF neuron) of 34 did not contain a power law relationship when the time series contained >1,500 spikes. As shown in Fig. 3, the percentage of neurons (pooled for all medullary regions and patterns of SND) with a power law relationship in their Fano factor curve was directly related to the number of spikes collected (sample size). In all but one case, the power law relationship was eliminated by random shuffling of the ISIs. The exception is described later in the text.

Examples of Fano factor curves for neurons with sympathetic nerve–related activity that were located in medullary regions other than the RVLM are shown in Figs. 4 and 5. In

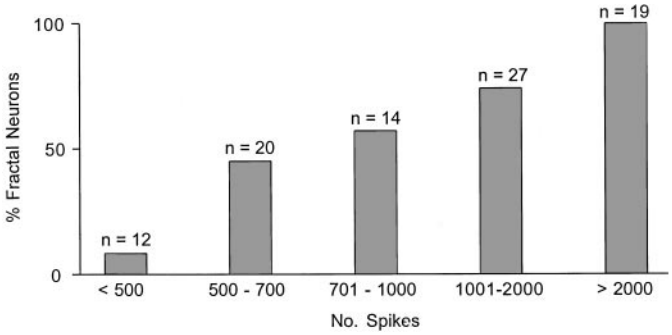

FIG. 3. The percentage of neurons with sympathetic nerve–related activity (pooled for all medullary regions) having a power law relationship in their Fano factor curve is plotted as a function of the number of spikes in the time series.

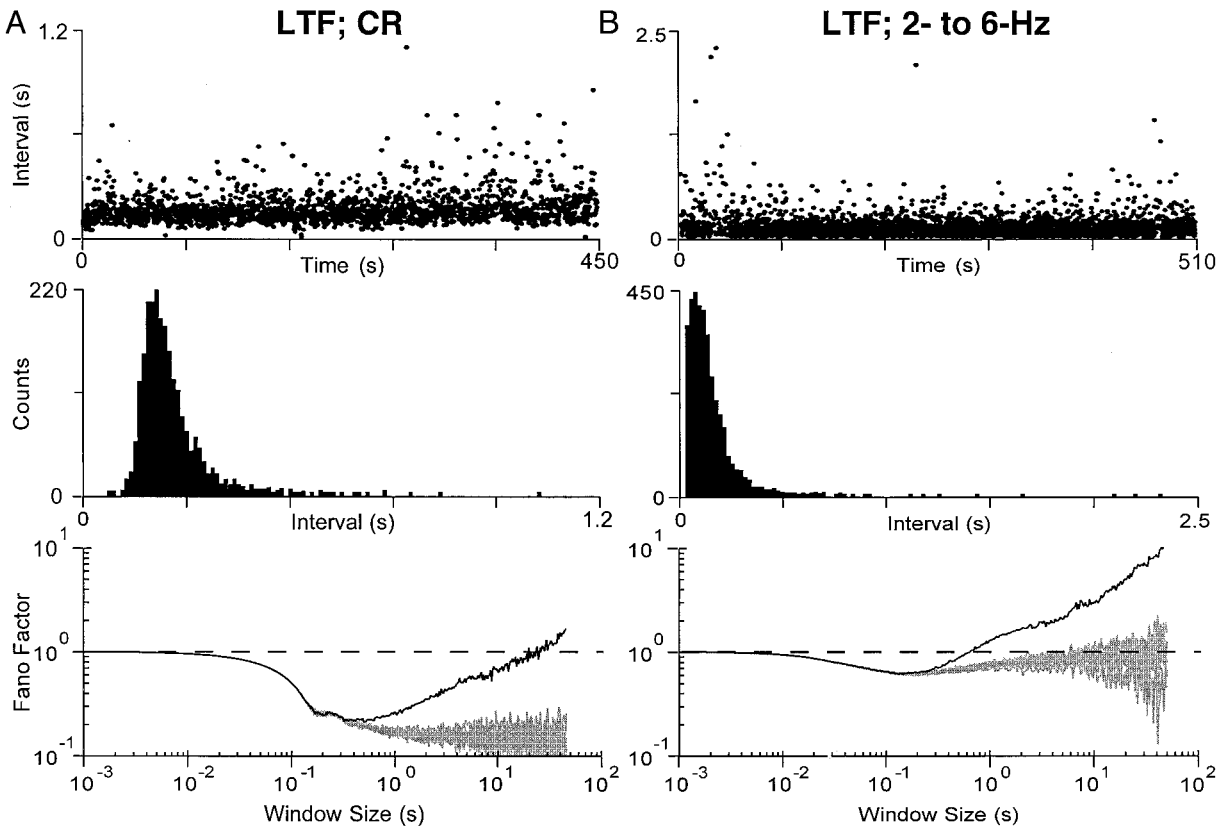

FIG. 4. Fano factor analysis of the spike trains of 2 neurons in the medullary lateral tegmental field (LTF), one (*A*) with activity correlated to the cardiac-related (CR) rhythm in SND and the other (*B*) with activity correlated to 2- to 6-Hz oscillations. Sequence of traces is same as in Fig. 2. Total counts in ISIHs is 2,312 in *A* and 3,510 in *B*. The shortest and modal ISIs were 54 and 170 ms, respectively, in *A* and 25 and 70 ms in *B*. Bin resolution (ISIHs) is 10 ms in *A* and 20 ms in *B*. Black line (*bottom*) is Fano factor curve for original spike train. Gray region is the superposition of the curves for 10 surrogate data sets.

each case, more than 2,000 spikes were collected. The Fano factor curve in Fig. 4*A* is for an LTF neuron whose naturally occurring spikes were correlated to the cardiac-related rhythm in SND of a baroreceptor-intact cat. The curve in Fig. 4*B* is for an LTF neuron with activity correlated to the irregular 2- to 6-Hz oscillations in a baroreceptor-denervated cat. In both of these cases, the power law relationship was eliminated by random shuffling of the ISIs. The Fano factor curve in Fig. 5 is for a CVLM neuron with activity correlated to the 10-Hz rhythm in SND of a baroreceptor-denervated cat. The curves for the surrogate data sets (gray region) in this case were atypical in that they show a power law relationship for window sizes ≥200 ms and Fano factor values that exceed one. Nevertheless, the slopes of the power law relationships for the 10 surrogate data sets were much reduced as compared with that of the curve for the original spike train (dark line). The clustering of relatively long intervals and of shorter intervals is particularly prominent in the time series of ISIs for this CVLM neuron (Fig. 5, *top*).

For six neurons with data sets containing >1,500 spikes, the ISIHs were multimodal rather than gamma-like in shape. This was the case for three LTF and one raphe neuron with activity correlated to the cardiac-related rhythm in SND and two RVLM neurons with activity correlated to the 10-Hz rhythm. For each of these spike trains, the primary mode in the ISIH corresponded to the period of the rhythm in SND or one of its multiples, and the Fano factor curve contained a power law relationship. The results illustrated in Fig. 6 are for one of the RVLM neurons with activity correlated to the 10-Hz rhythm in SND. Note the clustering of relatively long intervals near the end of 400-s time series of ISIs (Fig. 6, *top*). The mode at 95 ms in the ISIH (Fig. 6, *middle*) corresponds to the period of the 10-Hz rhythm in SND, while that at 190 ms is twice as long. The small peak near 30 ms reflects couplets of spikes occurring during some 10-Hz bursts of SND. The Fano factor curve for the spike train (Fig. 6, *bottom*, dark line) dipped well below one for a range of window sizes including the modal intervals of 95 and 190 ms. As the window size was further increased, a power law relationship appeared with a slope of 0.64. This relationship was eliminated by random shuffling of the ISIs (see surrogate data sets).

The properties of the 33 data sets containing >1,500 spikes are summarized in Table 1. The neurons are grouped according to the medullary region in which they were located and the component of SND to which their discharges were correlated. Values for each property are means with ranges in parentheses. Although the number of neurons in most groups is small, there was one noteworthy regional difference in the slopes of the power law relationships. As demonstrated by using the Student's *t*-test for unpaired data, the average slope of the power law relationship in the Fano factor curves for RVLM neurons with activity correlated to the cardiac-related rhythm was significantly steeper than that for LTF neurons with a corresponding relationship to SND ($P = 0.02$). There were no statistically

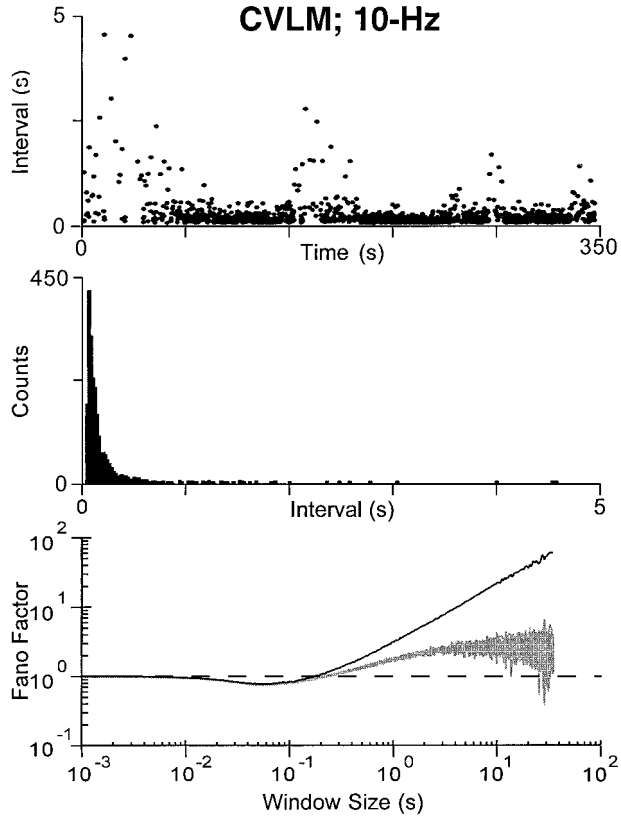

FIG. 5. Fano factor analysis of the spike train of a neuron in the caudal ventrolateral medulla (CVLM) with activity correlated to the 10-Hz rhythm in SND. Sequence of traces is same as in Fig. 2. The ISIH contains 2,128 counts and has a bin resolution of 20 ms. The shortest and modal ISIs were 35 and 45 ms, respectively. Black line (*bottom*) is the Fano factor curve for original spike train. Gray region is the superposition of the curves for 10 surrogate data sets.

significant differences in slopes for neurons located in the same region with activity correlated to different patterns of SND. For example, the average slope of the power law relationship for RVLM neurons with activity correlated to the cardiac-related rhythm was no different from those for RVLM neurons with activity correlated to the 2- to 6-Hz oscillations or 10-Hz rhythm. Our statistical comparisons did not include the raphe neurons due to the very small number of observations for time series containing ≥1,500 spikes.

Other statistical properties of spike trains

For a sample limited to 15 RVLM neurons (same as those in Table 1), we calculated the mean ISI and ISI variance for segments of the time series containing different numbers of intervals. This was done initially for the first four ISIs in the spike train and then repeated each time the number of intervals was increased by one. The final calculations were based on the total number of intervals in the time series. The mean ISI and ISI variance increased as a function of segment size (number of intervals counted) for two of the three RVLM neurons with activity correlated to the 10-Hz rhythm in SND, three of seven RVLM neurons with activity correlated to the cardiac-related rhythm, and three of five RVLM neurons with activity correlated to irregular 2- to 6-Hz oscillations. The example in Fig. 7*A* is for an RVLM neuron with activity correlated to the cardiac-related rhythm. In contrast, the mean ISI and ISI variance converged to stable values as the segment size was increased for the remaining RVLM neurons. The example in Fig. 7*B* is for an RVLM neuron with activity correlated to the cardiac-related rhythm in SND.

Spike trains of neurons without sympathetic nerve–related activity

In four cats anesthetized with Dial-urethan, we analyzed the spike trains of 29 neurons in the CVLM, LTF neurons, and RVLM whose discharges were not correlated to inferior cardiac SND (as demonstrated by spike-triggered averaging). The number of spikes in the time series (409–1,064 s in length) ranged from 2,115 to 12,606. The mean discharge rate of the neurons was 10.1 spikes/s (range, 1.9–38.3 spikes/s). The ISIHs of 23 of the neurons were gamma-like in shape, and the remainder were either bimodal or multimodal. The Fano factor curves for the majority of neurons contained a power law relationship for a wide range of window sizes exceeding the modal ISI. This was the case for 10 of 15 CVLM neurons, 8 of 11 LTF neurons, and 2 of 3 RVLM neurons. The slopes of the power law relationships ranged from 0.28 to 0.92. The power law relationship was eliminated by random shuffling of the ISIs in all but two cases. In the two exceptional cases (both CVLM neurons), the slope (0.86 and 0.89) of the power law relationship was unchanged by shuffling the ISIs. Thus the power law relationship in these cases could not be attributed to long-term

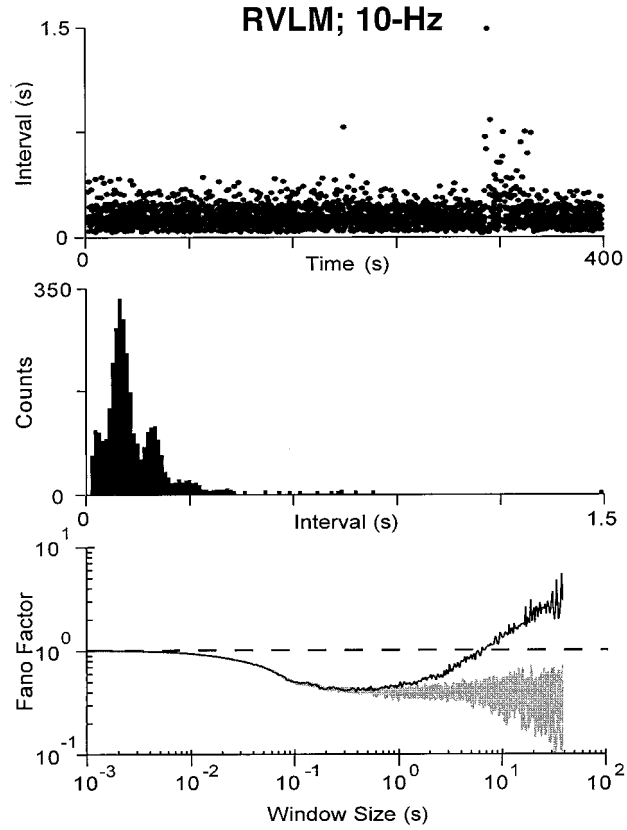

FIG. 6. Fano factor analysis of the spike train of an RVLM neuron with activity correlated to the 10-Hz rhythm in SND. Sequence of traces is same as in Fig. 2. The multimodal ISIH contained 3,837 counts and has a bin resolution of 10 ms. The shortest ISI was 15 ms; the modal intervals were 30, 95, and 190 ms. Black line (*bottom*) is the Fano factor curve for original spike train. Gray region is the superposition of the curves for 10 surrogate data sets.

TABLE 1. *Properties of spike trains of single medullary neurons with activity correlated to the CR rhythm, 10-Hz rhythm, or 2- to 6-Hz oscillations in sympathetic nerve discharge*

	n	Number of Spikes	Data Length, s	Spikes/s	Maximum ISI, s	Fano Slope
			RVLM neurons			
10-Hz rhythm	3	3,000 (1,974–3,837)	453 (397–565)	7.1 (3.5–9.7)	4.308 (1.484–7.871)	0.75 (0.64–0.93)
CR rhythm	7	1,832 (1,510–2,370)	647 (277–1,001)	2.5 (0.9–5.4)	2.413 (1.181–3.319)	0.78 (0.72–0.94)*
2- to 6-Hz oscillations	5	2,095 (1,694–2,587)	1,021 (487–1,802)	2.6 (1.3–5.3)	6.746 (0.750–16.897)	0.72 (0.64–0.91)
			Raphe neurons			
CR rhythm	1	2,401	1,007	2.4	2.753	0.7
2- to 6-Hz oscillations	2	2,742 (1,536–3,947)	1,073 (602–1,544)	3.8 (1.0–6.5)	4.804 (0.623–8.984)	0.67 (0.39–0.95)
			CVLM neurons			
10-Hz rhythm	4	2,279 (1,980–2,869)	339 (324–351)	6.7 (5.9–8.2)	2.185 (1.307–4.563)	0.83 (0.80–0.86)
			LTF neurons			
CR rhythm	9	2,468 (1,516–4,241)	537 (327–704)	4.8 (2.2–7.7)	2.562 (1.052–5.144)	0.57 (0.30–0.89)
2- to 6-Hz oscillations	2	2,713 (1,635–3,791)	390 (274–507)	6.8 (6.0–7.5)	2.450 (1.699–3.202)	0.39 (0.31–0.47)

Values are means with ranges in parentheses for time series containing ≥1,500 spikes. CR, cardiac related; ISI, interspike interval; RVLM, rostral ventrolateral medulla; CVLM, caudal ventrolateral medulla; LTF, medullary lateral tegmental field. * Significantly different from value for LTF neurons with activity correlated to the cardiac-related rhythm in sympathetic nerve discharge.

correlations among the ISIs. In the nine cases in which a power law relationship was absent, values of the Fano factor dipped below one, and the curve did not diverge from those for the 10 surrogate data blocks.

DISCUSSION

We found a power law relationship in the Fano factor curves for all but 1 of 34 medullary neurons with sympathetic nerve–related activity whose time series contained ≥1,500 spikes and for each of 19 neurons whose spike trains contained ≥2,000 spikes. This was the case independent of anatomical location and the component of SND to which unit activity was correlated. A power law relationship in the Fano factor curve raises the possibility that the process under study is statistically self-similar and, thus, fractal in nature (Bassingthwaighte et al. 1994; Liebovitch 1998). Self-similarity in spike trains means that its features measured at different temporal resolutions are related. Thus, in contrast to a renewal process in which the ISIs are independent of each other, fractal spike trains are characterized by long-term correlations among ISIs.

Before one can conclude that long-term correlations existed among ISIs, the possibility that the power law relationship simply reflected the distribution of the ISIs (shape of ISIH) must be eliminated (Teich and Lowen 1994; Teich et al. 1996). One way to distinguish between these alternatives is to shuffle the ISIs in a random manner and then plot the Fano factor curve for the surrogate data set. The original spike train and its surrogate data sets have identical ISIHs, but long-term correlations among the ISIs are destroyed by the shuffling process.

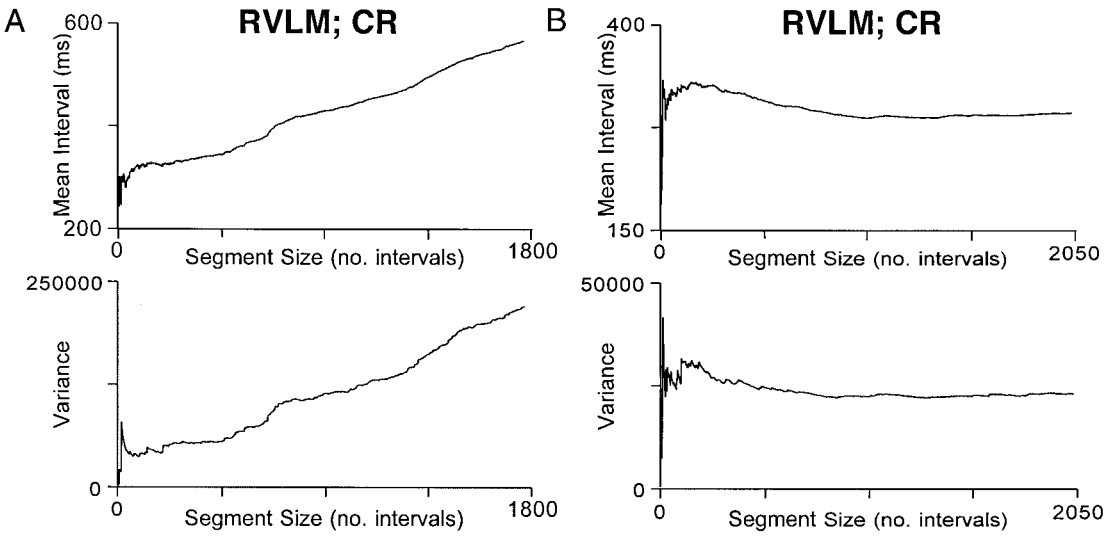

FIG. 7. Mean ISI and ISI variance is plotted as a function of the number of intervals counted (segment size) for 2 RVLM neurons (*A* and *B*) with activity correlated to the cardiac-related (CR) rhythm in SND.

That is, the surrogate data set approximates a renewal process in which the ISIs are independent of each other. For neurons with sympathetic nerve–related activity, shuffling of the ISIs eliminated the power law relationship in 32 cases and markedly reduced its slope in one case. The number of spikes collected was >1,500 in each of these cases. On this basis, we conclude that the power law relationships reflected long-term correlations of the ISIs rather than the distribution of the intervals. It follows that the variable ISIs of medullary neurons with activity correlated to SND arise, at least in part, from a fractal rather than a random generating process.

Other statistical properties of some of the spike trains support the notion that they can be viewed as fractal point processes. As dictated by the Central Limit Theorem, the moments (mean and variance) of a Gaussian distribution converge to stable values as the number of events counted is increased. In contrast, statistical self-similarity implies that the mean and variance keep changing as more and more data are analyzed (Liebovitch 1998). Thus the moments of a fractal process measured at one level of resolution may be different from those measured at other resolutions. Such cases are characteristic of a type of statistical fractal process called a stable Lévy process (Bassingthwaighte et al. 1994). We found that the mean ISI and ISI variance increased as a function of the number of intervals counted for 8 of 15 RVLM sympathetic neurons whose Fano factor curves contained a power law relationship. This reflects the increased probability of finding clusters of long intervals in the case of the mean and clusters of long and short intervals in the case of variance as more data are analyzed. Such clustering is inherent to fractal time series (Leibovitch 1998; Teich 1989). The spike trains of the other seven RVLM sympathetic neurons had moments that converged to stable values as the number of intervals counted was increased. Nevertheless, we believe that these spike trains also contained a fractal component because the power law relationship in the Fano factor curves was eliminated by random shuffling of the ISIs.

The percentage of neurons with sympathetic nerve–related activity having a fractal component in their spike train increased to 97% for time series containing ≥1,500 spikes and reached 100% for time series containing ≥2,000 spikes (see Fig. 3). Thus we presume that the lower percentages for time series containing fewer spikes does not mean that there are two separate populations of such neurons, one with and one without fractal spike trains. Rather, our results suggest that the spike trains of all RVLM, CVLM, LTF, and medullary raphe neurons with sympathetic nerve–related activity have fractal properties. The fractal behavior of some neurons may have been obscured by stochastic and/or rhythmic components of the spike train when the sample size was relatively small. These components might also influence the slope of the power law relationship in the Fano factor curve in instances when fractal behavior was clearly demonstrated. Thus whether the difference in slopes for RVLM and LTF neurons with activity correlated to the cardiac-related rhythm in SND (Table 1) is attributable to inherently different fractal characteristics among neuronal populations remains problematic.

Long-term correlations among ISIs reflecting a fractal point process might arise from properties inherent to the neurons themselves or of the network in which they are embedded. Evidence has been presented that ion channel opening and closing times in corneal endothelial cells have power law scaling characteristic of a fractal process (Liebovitch and Koniarek 1992; Liebovitch and Toth 1991). In neurons, such properties might lead to long-term correlations among ISIs. West (1990) has offered an intriguing mechanism for fractal behavior based on nonlinear feedback that induces an output on a time scale different from that of the input. When the output is again fed back into the system as part of the input, it generates a new response on yet another time scale. Such a network property would result in statistical self-similarity across multiple time scales and, thus long-term correlations among ISIs. The fact that LTF, CVLM, RVLM, and raphe neurons with sympathetic nerve–related activity are interconnected (Barman and Gebber 1987, 1989; Barman et al. 1995) is consistent with this "network" scenario.

What are the physiological implications of the fractal firing patterns of medullary neurons with sympathetic-related activity? First, the fractal behavior of these neurons may play a role in generating or reinforcing the fractal component of heart rate variability (Goldberger and West 1987; Goldberger et al. 1996). If so, our findings might be relevant in helping to explain why heart rate variability is reduced in some forms of disease (Goldberger 1992; Goldberger et al. 1996). Second, the long-term correlations among the ISIs of these neurons suggest that sympathetic control mechanisms actually prevent the cardiovascular system from reaching a steady state. To paraphrase Goldberger et al. (1996), the classical theory of homeostasis, according to which stable physiological processes seek to maintain "constancy" should be extended to account for the dynamical, far from equilibrium properties of fractal processes. Fractal behavior might prevent excessive mode-locking (e.g., constancy of heart rate) that would restrict the responsiveness of the cardiovascular system to continually varying inputs.

A hotly debated topic among sensory neurophysiologists is how information is represented in the spike trains of single neurons. As reviewed by Koch (1999), one school of thought favors the view that the mean firing rate of a neuron measured in a time window of appropriate length is the primary variable involved. A second theory is that information is encoded in the intervals between spikes. To some extent, temporal coding could play a role in the transfer of information from the sympathetic nervous system to the heart. If so, the following would be expected. First, at a population level, postganglionic SND should be fractal in nature. Second, the fractal pattern of postganglionic SND should influence heart rate variability. These issues are open to future investigation.

In closing, fractal behavior appears to be a general characteristic of neurons with sympathetic nerve–related activity located in the RVLM, CVLM, LTF, and perhaps the medullary raphe. The implication of this finding is that long-term correlations exist among the ISIs. Thus the spike trains of these neurons do not fit the simple model of a stochastic point process. Fractal behavior was not restricted only to neurons with sympathetic nerve–related activity. In fact, fractal firing patterns were observed for the majority of CVLM, LTF, and RVLM neurons whose discharges were not correlated to SND. This is not surprising because fractal behavior is common to many systems. For example, Teich and colleagues (Teich 1989, 1992; Teich and Lowen 1994; Teich et al. 1996) have identified neurons with fractal firing patterns at multiple levels of the auditory and visual systems in cats. Fractal behavior, however, is not ubiquitous to all systems. For example, Teich

(1989, 1992) reported that the spike trains of primary vestibular neurons do not have fractal properties. Considering the functionally heterogeneous nature of the regions of the reticular formation explored in the current study, it was not unexpected to find mixed populations of "fractal" and "nonfractal" neurons whose discharges were uncorrelated to SND.

The authors thank S. M. Sykes for typing the manuscript.

This study was supported by National Heart, Lung, and Blood Institute Grants HL-13187 and HL-33266.

REFERENCES

BARMAN SM AND GEBBER GL. Sequence of activation of ventrolateral and dorsal medullary sympathetic neurons. *Am J Physiol Regulatory Integrative Comp Physiol* 245: R438–R447, 1983.

BARMAN SM AND GEBBER GL. Axonal projection patterns of ventrolateral medullospinal sympathoexcitatory neurons. *J Neurophysiol* 53: 1551–1566, 1985.

BARMAN SM AND GEBBER GL. Lateral tegmental field neurons of cat medulla: a source of basal activity of ventrolateral medullospinal sympathoexcitatory neurons. *J Neurophysiol* 57: 1410–1424, 1987.

BARMAN SM AND GEBBER GL. Lateral tegmental field neurons of cat medulla: a source of basal activity of raphespinal sympathoinhibitory neurons. *J Neurophysiol* 61: 1011–1024, 1989.

BARMAN SM AND GEBBER GL. Rostral ventrolateral medullary and caudal medullary raphe neurons with activity correlated to the 10-Hz rhythm in sympathetic nerve discharge. *J Neurophysiol* 68: 1535–1547, 1992.

BARMAN SM AND GEBBER GL. Subgroups of rostral ventrolateral medullary and caudal medullary raphe neurons based on patterns of relationship to sympathetic nerve discharge and axonal projections. *J Neurophysiol* 77: 65–75, 1997.

BARMAN SM, ORER HS, AND GEBBER GL. Caudal ventrolateral medullary neurons are elements of the network responsible for 10-Hz rhythm in sympathetic nerve discharge. *J Neurophysiol* 72: 106–120, 1994.

BARMAN SM, ORER HS, AND GEBBER GL. Axonal projections of caudal ventrolateral medullary and medullary raphe neurons with activity correlated to the 10-Hz rhythm in sympathetic nerve discharge. *J Neurophysiol* 74: 2295–2308, 1995.

BASSINGTHWAIGHTE JB, LIEBOVITCH LS, AND WEST BJ. *Fractal Physiology*. New York: Oxford Univ. Press, 1994, p. 11–44.

COHEN MI AND GOOTMAN PM. Periodicities in efferent discharge of splanchnic nerve of the cat. *Am J Physiol* 218: 1092–1101, 1970.

COX DR AND LEWIS PAW. *The Statistical Analysis of Series of Events.* New York: Wiley, 1966, p. 17–36.

GEBBER GL, ZHONG S, LEWIS C, AND BARMAN SM. Differential patterns of spinal sympathetic outflow involving a 10-Hz rhythm. *J Neurophysiol* 82: 841–854, 1999.

GOLDBERGER AL. Fractal mechanisms in the electrophysiology of the heart. *IEEE Eng Med Biol* 11: 47–52, 1992.

GOLDBERGER AL, PENG C-K, HAUSDORFF J, MIETUS J, HAVLIN S, AND STANLEY HE. Fractals and the heart. In: *Fractal Geometry in Biological Systems. An Analytical Approach,* edited by Iannaconne PM and Khokha M. Boca Raton, FL: CRC, 1996, p. 249–266.

GOLDBERGER AL AND WEST BJ. Fractals in physiology and medicine. *Yale J Biol Med* 60: 421–435, 1987.

KOCH C. *Biophysics of Computation. Information Processing in Single Neurons.* New York: Oxford Univ. Press, 1999, p. 330–349.

KOCSIS B, GEBBER GL, BARMAN SM, AND KENNEY MJ. Relationships between activity of sympathetic nerve pairs: phase and coherence. *Am J Physiol Regulatory Integrative Comp Physiol* 259: R549–R560, 1990.

LIEBOVITCH LS. *Fractal and Chaos Simplified for the Life Sciences.* New York: Oxford Univ. Press, 1998, p. 74–77.

LIEBOVITCH LS AND KONIAREK JP. Ion channel kinetics. Protein switching between conformational states is fractal in time. *IEEE Eng Med Biol* 11: 53–56, 1992.

LIEBOVITCH LS AND TOTH TI. A model of ion channel kinetics using deterministic chaotic rather than stochastic process. *J Theor Biol* 148: 243–267, 1991.

TEICH MC. Fractal character of the auditory neural spike train. *IEEE Trans Biomed Eng* 36: 150–160, 1989.

TEICH MC. Fractal neuronal firing patterns. In: *Single Neuron Computation*, edited by McKenna T, Davis J, and Zormetzer SF. Boston, MA: Academic, 1992, p. 589–625.

TEICH MC AND LOWEN SB. Fractal patterns in auditory nerve-spike trains. *IEEE Eng Med Biol* 13: 197–202, 1994.

TEICH MC, TURCOTT RG, AND SIEGEL RM. Temporal correlation in cat striate-cortex neural spike trains. *IEEE Eng Med Biol* 15: 79–87, 1996.

TUCKWELL HC. *Introduction to Theoretical Neurobiology*: *Nonlinear and Stochastic Theories*. New York: Cambridge Univ. Press, 1988, vol. 2, p. 191–246.

WEST BJ. *Fractal Physiology and Chaos in Medicine*. Singapore: World Scientific, 1990, p. 67–78.